45

LA-UR- 01-3406

Approved for public release; distribution is unlimited.

c. /

Title: MESOSCALE MODELLING OF SHOCK INITIATION IN HMX-BASED EXPLOSIVES

Author(s): Roberta N. Mulford, NMT-15
Damian C. Swift, P-24

Submitted to: Proc American Physical Society Topical Conference on Shock Compression of Condensed Matter, to be held Atlanta GA, 25 to 29 Jun 01.

Los Alamos
NATIONAL LABORATORY

MESOSCALE MODELLING OF SHOCK INITIATION IN HMX-BASED EXPLOSIVES

Roberta N. Mulford and Damian C. Swift

E 530 Los Alamos National Laboratory, Los Alamos, New Mexico 87545

Hydrocode calculations are used to simulate initiation in single- and double-shock experiments on several HMX-based explosives. Variations in the reactive behavior of these materials reflects the differences between binders in the material, providing information regarding the sensitivity of the explosive to the mechanical properties of the constituents. Materials considered are EDC-37, with a soft binder, PBX-9501, with a relatively malleable binder, and PBX-9404, with a stiff binder. Bulk reactive behavior of these materials is dominated by the HMX component and should be comparable, while the mechanical response varies. The reactive flow model is temperature-dependent, based on a modified Arrhenius rate. Some unreacted material is allowed to react at a rate given by the state of the hotspot rather than the bulk state of the unreacted explosive, according to a length scale reflecting the hotspot size, and a time scale for thermal equilibration. The Arrhenius rate for HMX is assumed to be the same for all compositions. The initiation data for different HMX-based explosives are modelled by choosing plausible parameters to describe the reactive and dissipative properties of the binder, and hence the behavior of the hotspots in each formulation.

INTRODUCTION

We are developing reactive flow models intended to have a wide predictive capability covering composition and morphology, while being reasonably efficient for design simulations. Temperature-dependent reactions, based on an Arrhenius decomposition rate in the bulk explosive, could be used to reproduce aspects of the shock desensitisation observed in HMX-based explosives (1,2). The Arrhenius parameters were adjusted from the values obtained from thermal decomposition experiments (3) to reproduce shock initiation; the amount by which they were adjusted was less for better treatments of the microstructure. The most significant omission from the previous model was any explicit treatment of plastic work.

Here we present further additions to the microstructural model, and applications to HMX-based explosives where differences in the microstructure correlate with differences in initiation properties (4). This model has also been used to simulate highly non-ideal explosives (5)

REACTIVE FLOW MODEL

For continuum mechanics simulations, explosive material was represented as a heterogeneous mixture of components. Each component was represented by its volume fraction f, a thermodynamically complete equation of state (EOS), and a constitutive model if possible. (In the models used previously, the only components considered were 'unreacted explosive' and 'reaction products' with no distinction between explosive and binders.) The mixture was allowed to equilibrate in pressure and temperature, with an exponential relaxation rate towards the mean value. Pressure equilibration was assumed to be isentropic.

Local Arrhenius reaction rates were used,

$$\dot{\lambda} = R_0 \exp(-T^*/T), \qquad (1)$$

as this form is the most appropriate for chemical processes. An additional hotspot term was included, whereby material at the surface of reactive components was burnt at the temperature of the adjacent component. The area of pairs of components in contact with each other were expressed as functions of their volume fractions.

The increased plastic flow around internal pores was modelled by simulating the evolution of the state of the component adjacent to the pore, as well as its bulk state. The velocity gradient tensor applied to the pore wall was modelled as

$$\operatorname{grad}\vec{u}_{\text{wall}} = \chi(\rho/\rho_0) M \operatorname{grad}\vec{u}_{\text{bulk}}, \qquad (2)$$

where M is a 3×3 strain mapping matrix and $\chi(\rho/\rho_0)$ a compression factor. This model can be used to simulate hotspots originating from shear bands or brittle failure rather than bulk plastic work, by modifying the form of the equation or the values of its parameters.

CALIBRATION AND POP PLOTS

Thermodynamically complete EOS for condensed components were estimated from a mechanical EOS (generally obtained from shock wave data) and a constant heat capacity. A single point on the cold curve was estimated, and the mechanical EOS used to estimate the rest of the curve by integrating $p\,dv$ work. Steinberg's cubic Grüneisen form(6) was used to fit non-linear shock data.

The time constant τ_p for pressure equilibration was chosen by estimating the characteristic time for sound to pass a few times across a 'typical' grain in the microstructure. For HMX grains a few tens of μm in size, this implies that $\tau_p \sim 0.1\,\mu$s. The time constant τ_T for thermal equilibrium was estimated to be about an order of magnitude larger.

The density of common area between components i and j was estimated as

$$a_{ij} \propto f_i^{2/3} f_j^{2/3}, \qquad (3)$$

normalised to the approximate value

$$a(1/2, 1/2) = 4\pi r^2 n \qquad (4)$$

where r is the particle diameter in a mixture of two components of equal sizes and n is the number density of particles, estimated from the grain size.

The model of plasticity enhancement around a pore was calibrated against a simplified treatment of constant volume compression of a hollow shell. In this case,

$$\chi(\rho/\rho_0) = \left[1 - \frac{\rho}{\rho_0}(1 - \nu_0)\right]^{-1/3} \qquad (5)$$

where ν_0 is the initial porosity.

Common components

The EOS for HMX was estimated from Hugoniot data(8,7) and thermal properties.(3) An elastic-plastic constitutive model was used, based on observed values of the shear modulus and yield stress.(11)

Little useful data were found on NC or the binders used in the explosives considered. An EOS was estimated for polyurethane, again using Hugoniot data(7) and a 'typical' heat capacity for polymers.(9) This EOS was used for all binder components. The EOS for NC was estimated by assuming the same Hugoniot data as for cellulose acetate(7) but taking a solid density of 1.65 g/cm^3.(10)

The constitutive behaviour of the binder was treated implicitly by altering the plastic enhancement of deformation in the HMX. The stiffer the binder, the greater the enhancement used.

Initial estimates of the Arrhenius parameters were taken from calorimetry data,(3) and adjusted to reproduce initiation data. The parameters for HMX were adjusted by considering PBX 9501 data, as this composition does not have a reactive binder. In some simulations, the decomposition of the binder was modelled using a slow Arrhenius process; this made little difference to the initiation behaviour predicted. Initiation was not expected to be sensitive to the flame speed used for hotspot burn. This was verified by sensitivity studies.

Porous materials were represented as before by starting with a non-zero volume fraction of the reaction products at the STP state.

PBX 9501

PBX 9501 consists of 95% HMX, 2.5% estane and 2.5% BDNPA by weight, with a porosity ~1.6%.(3) The binder is fairly soft.

Simulations were made to investigate the sensitivity of shock initiation to the Arrhenius parameters. The simulations were compared with experimental Pop plots.(3) It was found possible to reproduce the experimental data to within $\sim$% in pressure with $T^* = 24000\,\mathrm{K}$ and $R_0 = 10^{10}/\mu\mathrm{s}$ ('model A'). This value of T^* is much closer to the value deduced from calorimetry data (26500 K(3)) than was achieved previously. R_0 is considerably smaller than the $10^{13}/\mu\mathrm{s}$ value from calorimetry, but is more plausible as an atomic vibration frequency. Run distances were generally much less sensitive to the reaction rate than was found previously, apparently because of the more explicit treatment of the different components of the explosive rather than the inclusion of plastic work. Pop plots could be obtained which were similar to model A over a restricted range of pressures using quite different values of the Arrhenius parameters: $T^* = 23000\,\mathrm{K}$, $R_0 = 5 \times 10^9/\mu\mathrm{s}$ for model B, and $T^* = 23000\,\mathrm{K}$, $R_0 = 10^{10}/\mu\mathrm{s}$ for model C. (Fig. 1.)

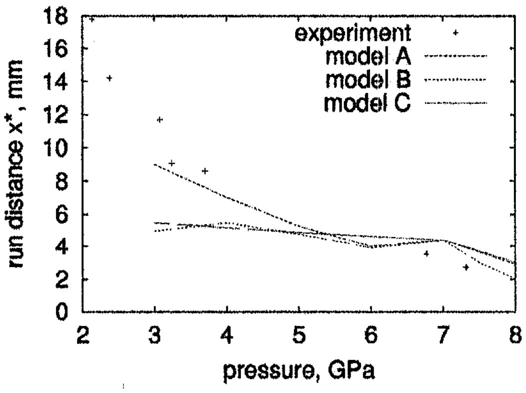

FIGURE 1. Run distance to detonation for PBX 9501.

PBX 9404

PBX 9404 consists of 94% HMX, 3% NC, and 3% CEF by weight, with a porosity $\sim$1.6%.(3) The binder is relatively stiff.

Simulations were made based on model A for PBX 9501 but with the correct composition and a higher plastic enhancement. The predicted Pop plot was not significantly different, consistent with experiment.(3) It was not found necessary to adjust the Arrhenius parameters for NC away from the values deduced from calorimetry. (Fig. 2.)

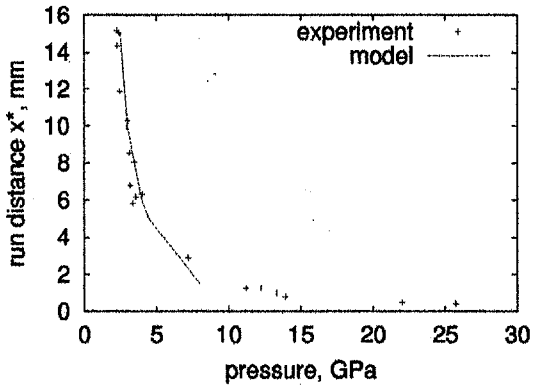

FIGURE 2. Run distance to detonation for PBX 9404.

EDC37

EDC37 consists of 91% HMX, 8% K10, and 1% NC by weight, with a porosity $\sim$0.18%.(4) The binder is liquid.

Simulations were made based on model A for PBX 9501 but with the correct composition and plastic enhancement removed. If no other changes were made, the predicted Pop plot was similar to the PBX compositions, in contrast with experimental data where EDC37 is significantly less sensitive.(4) The simulations were brought into closer agreement with experiment by reducing the time scales for equilibration to $\tau_p = 10^{-2}\,\mu\mathrm{s}$ and $\tau_T = 0.1\,\mu\mathrm{s}$. This change can be rationalised on the basis of smaller pores in EDC37, commensurate with the lower porosity. (Fig. 3.)

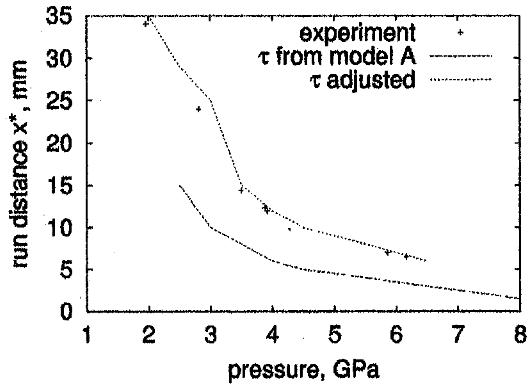

FIGURE 3. Run distance to detonation for EDC37.

PARTICLE VELOCITY HISTORY

Pop plots are an integrated measure of the initiation of an explosive, and it is a far more sensitive discriminant to compare the velocity history at different points in the explosive during the build-up to detonation.

Experimental measurements were obtained in 1D gun-driven impactor experiments, using electromagnetic gauges to record the particle velocity history at Lagrangian positions in the explosive sample.(4)

Comparisons were made against PBX 9501 initiated by a single and a double shock.(12) The new reactive flow model reproduced the details of the initiation history more accurately than the old model, though the velocity history still increased somewhat more abruptly than was found experimentally. (Fig. 4.)

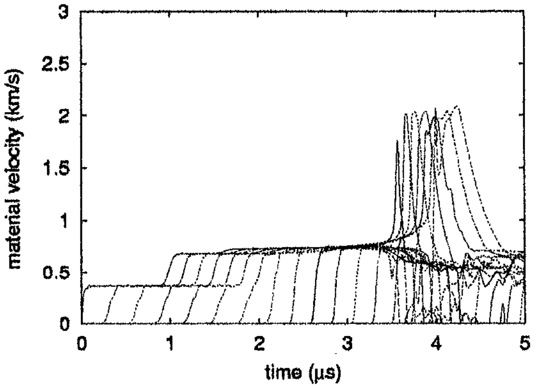

FIGURE 4. Simulated gauge data for PBX-9501, compared with experiment.

CONCLUSIONS

The reactive flow model described previously was extended to describe each component of the explosive explicitly, and to include inhomogeneous plastic heating as a contribution to hotspots. The new model was able to reproduce the measured Pop plot for PBX 9501 using Arrhenius parameters much closer to the values deduced from calorimetry, suggesting that the model contains essentially all the physics necessary to treat shock initiation in a predictive way.

Pressure and temperature equilibrium parameters were specified explicitly rather than calculated from the microstructure. If adjusted to reflect different microstructures, the model was reasonably accurate in predicting the initiation properties of PBX 9404 and EDC37. The new model also matched particle velocity histories more accurately.

The contribution of inhomogeneous plastic heating seemed less important than the explicit treatment of each condensed component, possibly because the elastic-plastic constitutive model underpredicted the heating around a pore.(13)

REFERENCES

1. R N Mulford and D C Swift, ***Reactive flow models for the desensitisation of high explosives***, Proc International Workshop on Non-Ideal Explosives, held Socorro, New Mexico, USA, Mar 1999, EMRTC (2000).
2. R N Mulford and D C Swift, ***Reactive flow models for the desensitisation of high explosives***, Proc APS SCCM 1999, AIP (2000).
3. T.R. Gibbs and A. Popolato, "LASL Explosive Property Data" University of California Press, Berkeley (1980).
4. R.L. Gustavsen, S.A. Sheffield, R.R. Alcon, L.G. Hill, R.E. Winter, D.A. Salisbury and P. Taylor, ***Initiation of EDC37 measured with embedded electromagnetic particle velocity gauges***, Proc APS SCCM 1999, AIP (1999).
5. R.N. Mulford and D.C. Swift, ***Temperature-based reactive flow models for ANFO***, Proc International Workshop on Non-Ideal Explosives, held Socorro, NM, May 2001.
6. D C Swift, ***Steinberg-Style Grüneisen Equations of State for Cerium, Lanthanum and Scandium***, Los Alamos National Laboratory report LA-UR-01-3005 (2001).
7. S P Marsh (Ed), "LASL Shock Hugoniot Data", University of California (1980).
8. M. van Thiel, *Compendium of Shock Wave Data*, Lawrence Radiation Laboratory report UCRL-50108 (1966).
9. J.A. Dean, "Lange's Handbook of Chemistry" (13th ed.), McGraw-Hill (1972).
10. R. Rabie (Los Alamos National Laboratory), private communication (2001).
11. J.J. Dick, A.R. Martinez and R.S. Hixson, ***Plane impact response of PBX 9501 below 2 GPa***, Proc 11th International Detonation Symposium, ONR 33300-5 (2000).
12. R.N. Mulford (Los Alamos National Laboratory), unpublished gas gun data.
13. N.J. Whitworth and J.R. Maw, ***Modelling 'hot-spot' initiation in heterogeneous high explosives***, Proc APS SCCM 1999, AIP (1999).

Mesoscale Modelling of Shock Initiation in HMX-Based Explosives

R.N. Mulford and D.C. Swift

Los Alamos National Laboratory
Los Alamos, NM 87545, USA

Outline

- Motivation
- Model:
  - Equations of state
  - Constitutive models
  - Reaction rates
- Calibration and performance:
  - PBX 9501 run distance
  - PBX 9404 run distance
  - EDC37 run distance
  - PBX 9501 velocity history

Motivation: predictive capability

Want to predict initiation and detonics given:

- Variations in composition
- Variations in morphology
- Different loading conditions

Previous work on PBX and ANFO: need physically-based model rather than just mechanical calibrations.

Overview of model

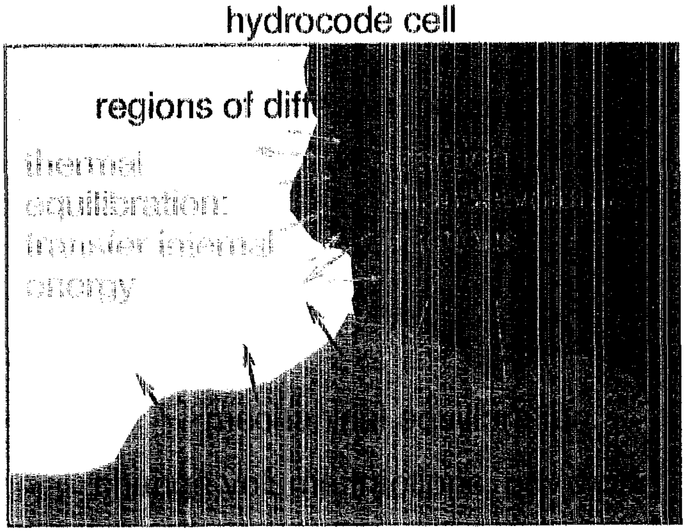

- Equation of state + constitutive model for each component (spatial region).
- Equilibration process for temperature and pressure.
- Strain enhancement around pores ⇒ extra plastic heating.
- Chemical reactions transfer mass between components.
- Regions may include multiple reacting chemicals.

Condensed-phase equations of state

- Need accurate temperature ⇒ thermodynamically complete.
- Want to use QM EOS or harmonic model.
- Stop-gap: mechanical EOS + reference curve + heat capacity.
- Cold curve deduced from mechanical EOS fitted to shock data, with $\Gamma(\rho)$ model for off-Hugoniot states.
- Assumed value for $\rho(p=0, T=0)$ or $e(\rho=\rho_{\mathrm{STP}}, T=0)$ – not particularly sensitive.
- Assumed constant c_v.

Constitutive model

For bulk of each component (where available):

- State: EOS (ρ, e) + elastic strain deviator + scalar plastic strain.
- Elastic – plastic model used here.

Hotspot surface burn

Subcell model:

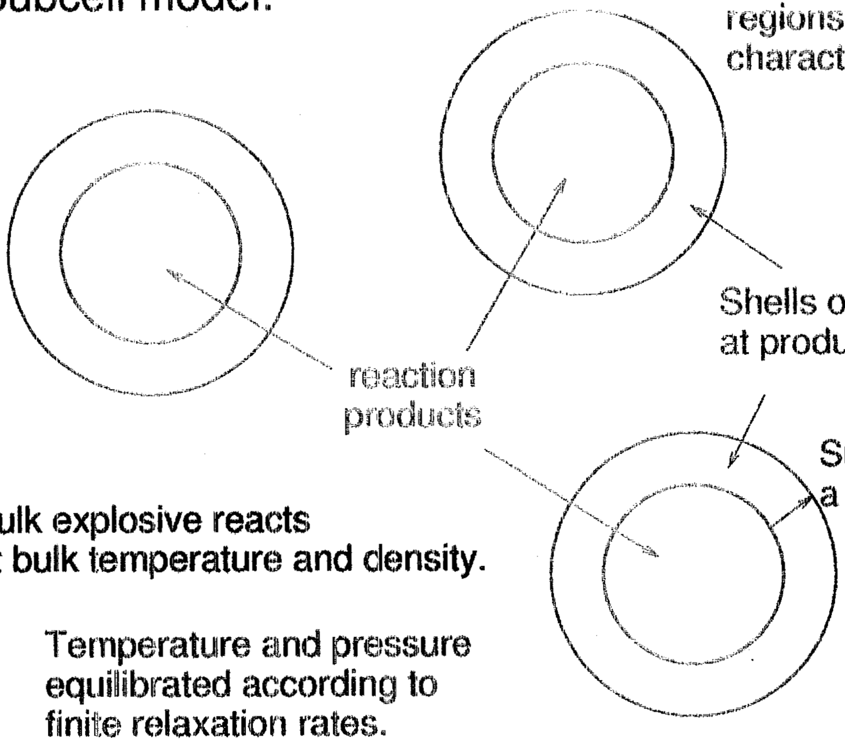

Reaction products occupy
regions of a single
characteristic size.

Shells of explosive reacting
at products' temperature

reaction
products

Surface burns with
a flame speed,
function of density
and temperature.

Bulk explosive reacts
at bulk temperature and density.

Temperature and pressure
equilibrated according to
finite relaxation rates.

Enhanced plastic strain around pores

Subcell model:

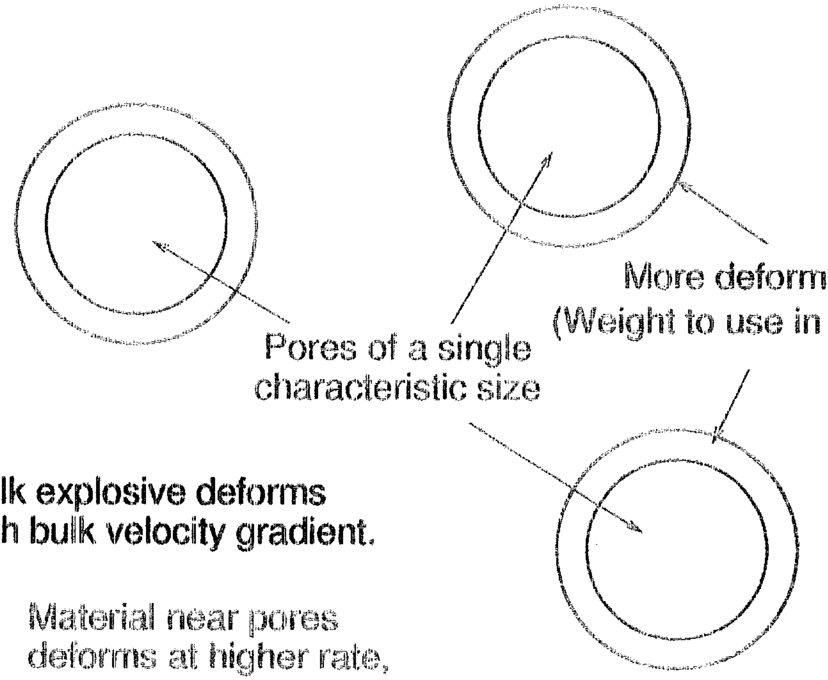

More deformation => hotter.
(Weight to use in bulk reaction rate.)

Pores of a single
characteristic size

Bulk explosive deforms
with bulk velocity gradient.

Material near pores
deforms at higher rate,
depending on compression.

Velocity gradient (tensor) applied to bulk (component): grad $\vec{u}$.

Internal pore ⇒ variation in grad $\vec{u}(\vec{r})$.

Consider grad $\vec{u}$ at wall or pore:

$$\text{grad}\,\vec{u}_{\text{wall}} = \chi(\rho/\rho_0)M\,\text{grad}\,\vec{u}_{\text{bulk}}$$

where M is 3×3 strain mapping matrix, χ is compression function.

Choose M, χ to represent different microstructures.

Calibration (general)

– pure-component properties + microstructure.

- Pressure equilibration time: ‘a few’ times sound transit time for a grain.

- Temperature equilibration time: ∼order of magnitude larger.

- Surface burn area: common area between components i and j

  $$a_{ij} \propto f_i^{2/3} f_j^{2/3},$$

  normalised to

  $$a(1/2, 1/2) = 4\pi r^2 n$$

  where r is grain diameter, n is grain number density.

- Enhanced plastic flow: estimated from constant volume compression of hollow shell,

  $$\chi(\rho/\rho_0) = \left[1 - \frac{\rho}{\rho_0}(1 - \nu_0)\right]^{-1/3}$$

  where ν_0 is initial porosity.

Calibration (components)

- HMX EOS: Steinberg-type Grüneisen fit to shock data, Gibbs & Popolato heat capacity + expansivity.
- Polyurethane EOS: Steinberg-type Grüneisen fit to shock data, Lange heat capacity. (Slow-reacting binders treated as polyurethane.)
- NC EOS: assumed $u_s - u_p$ for cellulose acetate (Grüneisen fit), took $\rho_0 = 1.65\,\mathrm{g/cm^3}$, estimated c_v.
- Products: temperature-dependent JWL for PBX 9404 – not sensitive for initiation.
- HMX reaction rate: calorimetry values from Gibbs & Popolato, adjusted to match PBX 9501 Pop plot.
- NC reaction rate: calorimetry values from Gibbs & Popolato.
- Slow-reacting binder rate: token value (not sensitive).
- Initial porosity: nonzero volume fraction of products, STP state.

PBX 9501: run distance

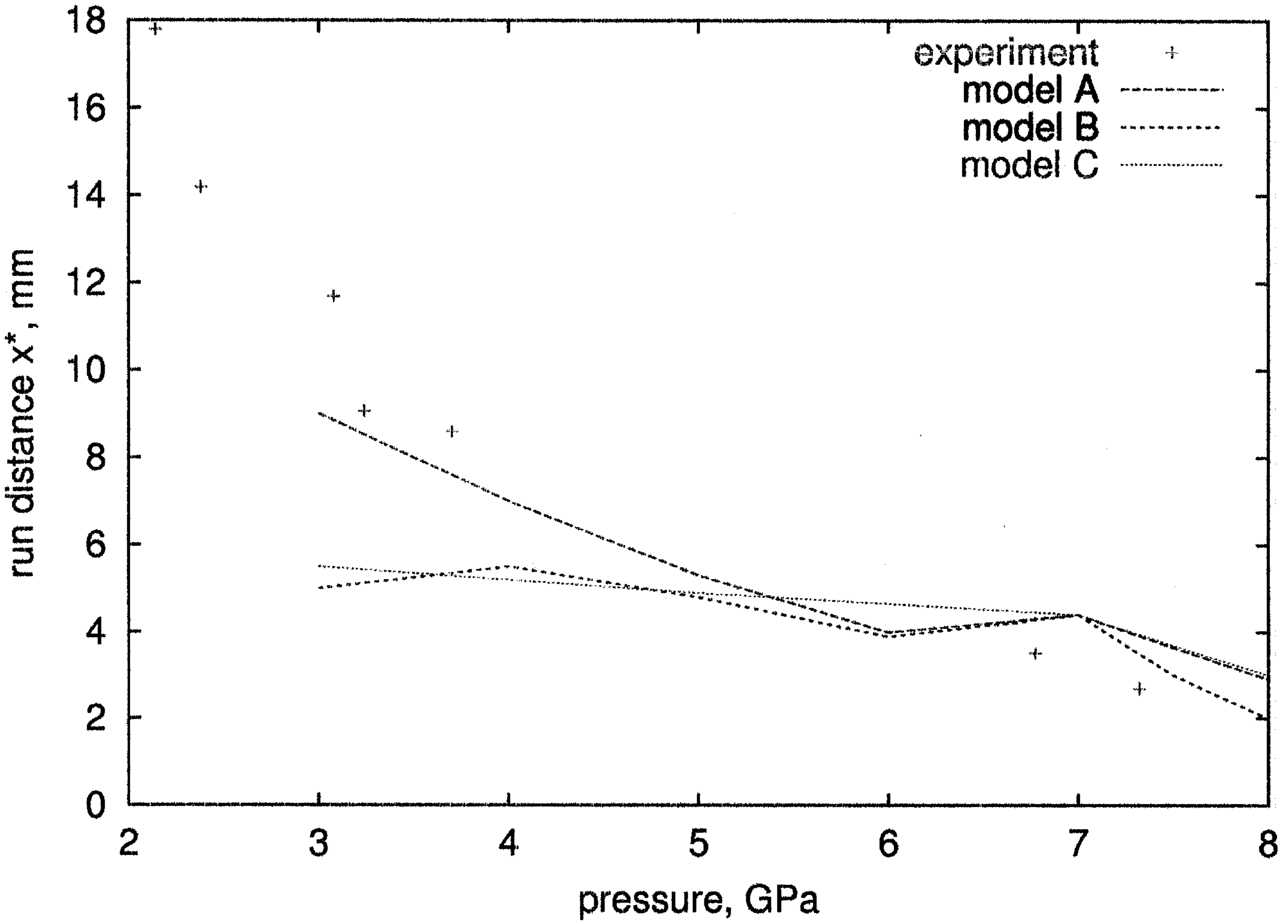

Model	T^* (K)	R_0 ($1/\mu s$)
A	24000	10^{10}
B	23000	5×10^9
C	23000	10^{10}

PBX 9404: run distance

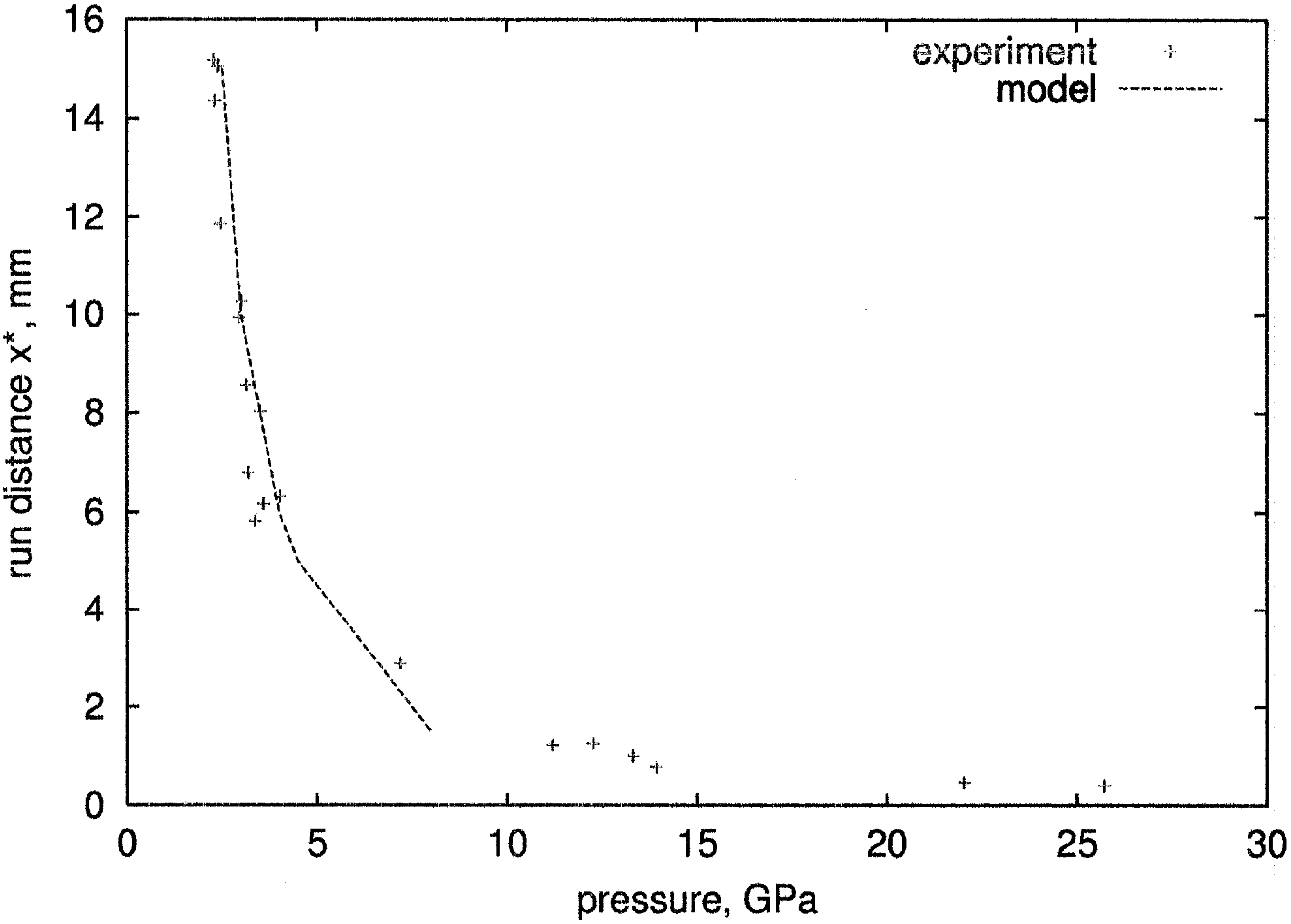

(Simulations used HMX Arrhenius parameters from PBX 9501 model A, with composition and plastic enhancement adjusted for PBX 9404.)

EDC37: run distance

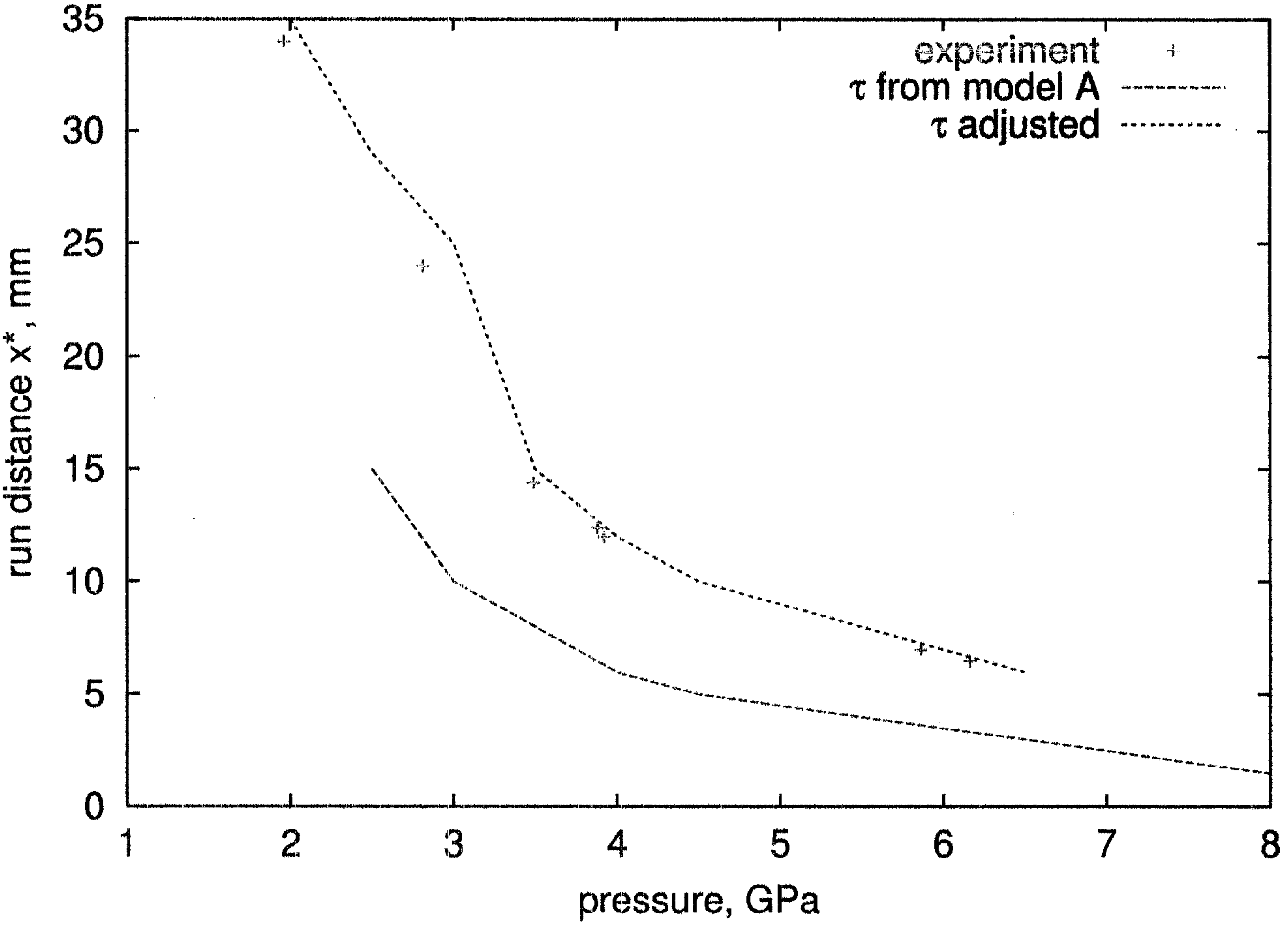

(Simulations used HMX Arrhenius parameters from PBX 9501 model A, with composition and plastic enhancement adjusted for EDC37.)

Model	τ_p (μs)	τ_T (μs)
A	0.10	1.00
adjusted	0.01	0.10

PBX 9501: particle velocity

Comparison with electromagnetic velocity gauge records from gas gun impact experiment.

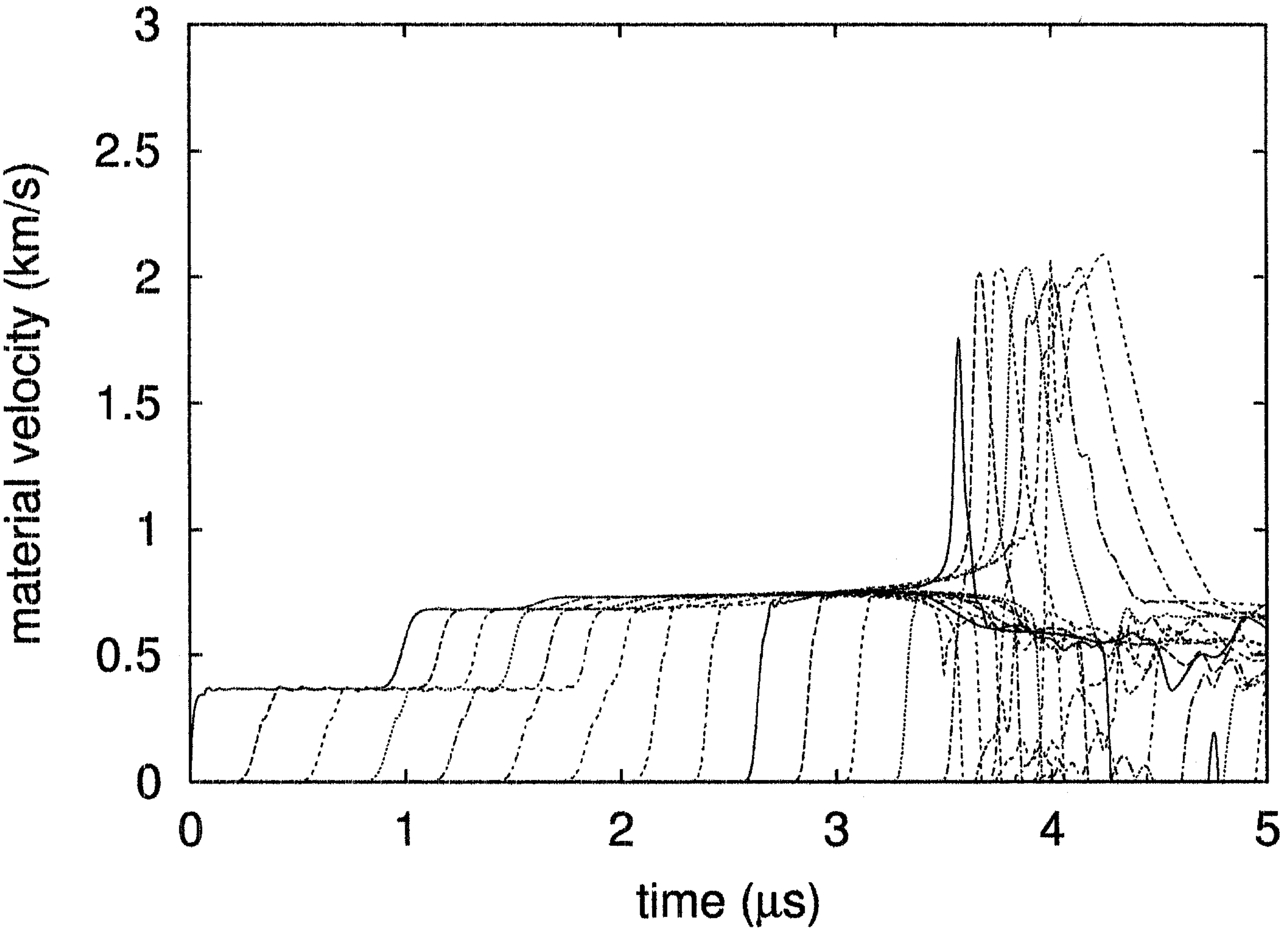

Summary and Conclusions

- Physically-based reactive flow model for HMX-based explosives.
- 'Coarse mesoscale' model of microstructure: physical constituents + heterogeneous effects.
- Heterogeneous effects: equilibration, surface burn, plastic enhancement.
- Model can predict effect of composition, porosity.
- Preliminary trials: reasonable for run distance and velocity history.
- Sufficient physics; need to refine models slightly.

Mesoscale Modelling of Shock Initiation in HMX-Based Explosives

R.N. Mulford and D.C. Swift

Los Alamos National Laboratory
Los Alamos, NM 87545, USA

Outline

- Motivation
- Model:
  - Equations of state
  - Constitutive models
  - Reaction rates
- Calibration and performance:
  - PBX 9501 run distance
  - PBX 9404 run distance
  - EDC37 run distance
  - PBX 9501 velocity history